Improving the Impedance-Based Stability Criterion by Using the Vector Fitting Method

Dowlatabadi, Mohammadkazem Bakhshizadeh; Blaabjerg, Frede; Hjerrild, Jesper; Kocewiak, Lukasz; Bak, Claus Leth

Published in:
I E E E Transactions on Energy Conversion

DOI (link to publication from Publisher):
10.1109/TEC.2018.2849347

Publication date:
2018

This article has been accepted for publication in a future issue of this journal, but has not been fully edited. Content may change prior to final publication. Citation information: DOI 10.1109/TEC.2018.2849347, IEEE Transactions on Energy Conversion

Improving the Impedance Based Stability Criterion by Using the Vector Fitting Method

Mohammad Kazem Bakhshizadeh, *Student Member, IEEE*, Frede Blaabjerg, *Fellow, IEEE*, Jesper Hjerrild, Łukasz Kocewiak, *Senior Member, IEEE*, and Claus Leth Bak, *Senior Member, IEEE*

***Abstract*--In this paper, some issues related to the impedance based stability criterion such as RHP poles in the minor loop gain, how to specify source and load impedances, and node-dependent stability margins are discussed and the vector fitting method is used to improve the method. This results in an eigenvalue analysis of the system instead of using the Nyquist diagram, and leads to obtain more information about the system. Furthermore, a participation factor analysis can be used to identify the problematic subsystem. The proposed method is examined in the assessment of a stable and an unstable system and simulation results are used for verification.**

***Index Terms*-- Eigenvalue analysis; Impedance; Harmonic stability; Power converter; Vector Fitting.**

I. Introduction

In harmonic stability studies, the stable operation of a system must be ensured at any possible configuration and if in some cases the stability margins are not enough, a solution (preferably a software solution such as retuning the controller gains to minimize the costs) should be found.

The Impedance Based Stability Criterion (IBSC) is widely used [1]–[4] to investigate the interaction between the power converters and passive elements. In this method the stability of a current controlled converter can simply be assessed by studying the Nyquist diagram for the minor loop gain *L*, which is the ratio of the grid (load) impedance and the converter (source) impedance as shown in Fig. 1.

$$L = \frac{Z_{load}(s)}{Z_{source}(s)} \quad (1)$$

The prerequisites of this method are: 1) the converter itself must be stable while unloaded (short-circuited to ground in case of a current controlled converter), 2) the grid itself must be stable when the converter is disconnected. It has been shown that for a power-electronic-based power system, which may have many power converters, the IBSC is a powerful method for ensuring stable operation [5], but it is not discussed how the load and source impedances should be chosen, or whether it is necessary to plot the Nyquist diagram for all converters for a full overview. In [6] it has been shown that the source and the load impedances should be selected based on the power flow direction in an HVDC back-to-back converter.

In a multi-converter system, other converters are grouped together with the grid as the load impedance. Therefore, the second precondition of the IBSC (the stability of the grid) might not be satisfied. If the load impedance becomes unstable, then, some Right Half Plane (RHP) poles will appear in the minor loop gain. Thus, the stability can simply not be evaluated by counting the number of encirclements due to the Nyquist Stability Criterion, which states the number of RHP poles of a closed loop system is equal to the number of times the Nyquist plot encircles the critical point (-1,0) **plus** the number of the RHP poles of the open loop gain [7]. In [8], [9] a step-by-step method is proposed to make sure that no RHP pole appears in the load impedance.

Another problem of the IBSC that has been reported in [10]–[12] is that relative stability margins such as Phase Margin (PM) and Gain Margin (GM) are dependent on where the IBSC is considered. In [11], [12] it has been shown that the eigenvalues of the system are independent of the measurement point and they can be used as a relative stability measure. The eigenvalues can be obtained by an analytical evaluation of the whole system [13] or by approximating the driving point impedance, which is indeed the equivalent impedance of that node as a frequency response, into state equations using the Vector Fitting method [11], [12]. However, the former leads to a very complicated study and it also needs analytical models of all components that might not be available due to the confidentiality or difficulty in the modeling [14]–[16]. The latter can also not identify the problematic subsystem because it only measures the driving

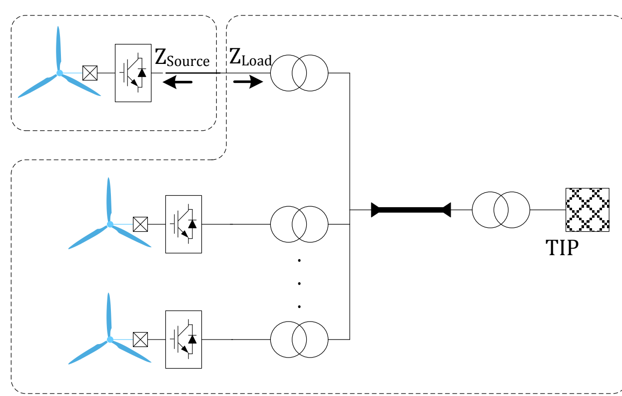

Fig. 1. Source and load impedances in a multi-converter system like a windfarm.

This work was supported in part by Ørsted Wind Power A/S and in part by Innovation Fund Denmark.

M. K. Bakhshizadeh, J. Hjerrild and Ł. Kocewiak are with Ørsted Wind Power A/S, Fredericia, Denmark (e-mail: modow@orsted.dk; jeshj@orsted.dk; lukko@orsted.dk).

F. Blaabjerg, and C. L. Bak are with the Department of Energy Technology, Aalborg University, Aalborg, Denmark (e-mail: fbl@et.aau.dk; clb@et.aau.dk).

This article has been accepted for publication in a future issue of this journal, but has not been fully edited. Content may change prior to final publication. Citation information: DOI 10.1109/TEC.2018.2849347, IEEE Transactions on Energy Conversion

point impedance. The method also assumes that the current configuration of the system is stable and uses some measurements either in simulations or in experiments. However, in the design phase the system designer might have some unstable cases, which cannot be predicted by this method. The Vector Fitting method has recently been used for finding a state-space model for the components, whose parameters/structures are unknown due to either the confidentiality or difficulty in the modeling [16]. The Component Connection Method (CCM) is afterwards used to find the overall state-space model of the entire system. However, the final matrices are of high order and the errors in identification of different components might be accumulated and affect the final results.

In this paper the eigenvalue-based stability criterion is combined with the IBSC. The differences with [11], [12] are: 1) it models the subsystems separately and therefore, the proposed method is able to determine which subsystem causes the instability mainly or where the changes have a significant effect on improving the condition; 2) it also works well in unstable systems, because the impedances that are fed into the method could be unstable. It must be noted that this method is a design phase study, where the designers are very interested to see and mitigate problems before commissioning in order to minimize the cost. Therefore, all components are known to the designer as detailed models or at least as frequency response data. This is the case for the terminal characteristics of Wind Turbine Generators or frequency domain models of cables and transformers. In [16] the entire system is modelled in detail and all dynamics of the system can be studied, whereas in this paper the system is studied from a node and in the end a reduced model of the system will be obtained. Multiple uses of the VF are avoided by doing this and the errors in the final results could be kept below a certain limit and identification is also less time-consuming. Furthermore, the idea presented in this paper can simply be implemented in power system softwares since it only needs two impedance frequency scans. Finally, in [16] the problematic component in the system can be found but in this paper the problematic subsystem is found. The problematic component can be found by repeating this procedure from different points. A case showing this is presented in section IV.

II. The Vector Fitting Method

The Vector Fitting (VF) method is an iterative way to find an approximated rational transfer function for a given numerical frequency response data [17]–[19]. The transfer function can be expressed as a sum of partial fractions

$$f(s) \approx \sum_{m=1}^{N} \left(\frac{R_m}{s-P_m}\right) + D + sE \tag{2}$$

where, R_m is the corresponding residue of the pole P_m. D is the feedthrough (direct input to output gain) matrix and E is non-zero in cases that the transfer function is not proper (the order of the numerator is higher than the denominator). Equation (2) can be represented by state-space equations as (3).

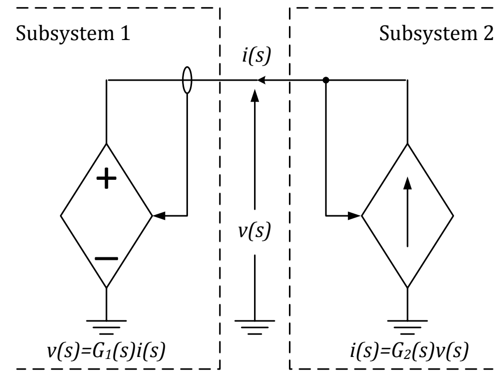

Fig. 2. The system is decomposed into two subsystems, one is represented by an impedance while the other one is modelled as an admittance.

$$\begin{cases} \dot{x} = Ax + Bu \\ y = Cx + Du + E\dot{u} \end{cases} \tag{3}$$

The passivity and stability enforcement are the processes, by which the passivity [20] (i.e. positive real part at all frequencies) and stability (i.e. all poles in the Left Half Plane) of the approximated model are ensured. However, these options are not used here because; 1) the passivity assumption for a converter admittance/impedance might not be true [21]; 2) the aim of this study is also to evaluate stability, and of course in some cases the system might be concluded to be unstable and further actions must be carried out to regain a stable and robust system.

III. The Proposed Method

In this method, the system is decomposed into two subsystems. One subsystem is modelled as an impedance system, where the terminal voltage is regulated based on the terminal current, while the other one is modelled as an admittance system, where the current is a function of the terminal voltage. Fig. 2 shows such a system, where Subsystem 1 is an impedance model and Subsystem 2 is an admittance model. The general state equations of the mentioned systems are

$$\begin{cases} \dot{x_1} = A_1 x_1 + B_1 i \\ v = C_1 x_1 + D_1 i + E_1 di/dt \end{cases} \tag{4}$$

$$\begin{cases} \dot{x_2} = A_2 x_2 + B_2 v \\ i = C_2 x_2 + D_2 v + E_2 \dot{v} \end{cases} \tag{5}$$

The impedance/admittance models can be chosen arbitrarily, however, they should be chosen in a way that at least the transfer function of one subsystem is proper. Otherwise the problem can be solved by swapping the roles of the two subsystems (admittance ↔ impedance) and by inverting the transfer functions. An improper transfer function tends to go to infinity as frequency increases. This can be used to visually estimate if a numerical data is from an improper transfer function. Alternatively, the results of the VF can also be used for this matter; if the identified model has a considerable E coefficient, then, the system under study is improper.

In order to find the whole system model first it is assumed that both transfer functions are proper (E_1 and E_2 matrices are Zero). Then, the two state equations can be combined into one

This article has been accepted for publication in a future issue of this journal, but has not been fully edited. Content may change prior to final publication. Citation information: DOI 10.1109/TEC.2018.2849347, IEEE Transactions on Energy Conversion

dynamical system as

$$\begin{bmatrix}\dot{x_1}\\ \dot{x_2}\end{bmatrix}=\begin{bmatrix}A_1 & 0\\ 0 & A_2\end{bmatrix}\begin{bmatrix}x_1\\ x_2\end{bmatrix}+\begin{bmatrix}B_1 & 0\\ 0 & B_2\end{bmatrix}\begin{bmatrix}i\\ v\end{bmatrix} \quad (6)$$

There are two equations for v and i, thus, they can be solved and expressed in terms of x_1 and x_2. Therefore, the dynamics of the system can be defined as

$$\begin{bmatrix}\dot{x_1}\\ \dot{x_2}\end{bmatrix}=[A_T]\begin{bmatrix}x_1\\ x_2\end{bmatrix}$$
$$=\begin{bmatrix}A_1+B_1\Gamma D_2C_1 & B_1\Gamma C_2\\ B_2(C_1+D_1\Gamma D_2C_1) & A_2+B_2D_1\Gamma C_2\end{bmatrix}\begin{bmatrix}x_1\\ x_2\end{bmatrix} \quad (7)$$

where, $\Gamma \overset{\text{def}}{=} (I-D_2D_1)^{-1}$ and I is the identity matrix of the appropriate size.

In [16] the CCM is used, which is unable to deal with improper transfer functions, but this problem is addressed here. If one of the subsystems is improper (e.g. $E_1<>0$ and $E_2==0$) then depending on whether subsystem 2 is strictly proper or not (D_2==0) different conditions exist:

1) If D_2 is a zero matrix, then

$$i=C_2x_2 \overset{d/dt}{\Longrightarrow} di/dt=C_2\dot{x_2}=C_2(A_2x_2+B_2v) \quad (8)$$

Now (8) can be replaced in (4) to remove the input derivatives in the state equations, and therefore, the same approach can be followed to eliminate the current and voltage from the equations and the new state matrix would be

$$A_T=\begin{bmatrix}A_1 & B_1D_1\\ B_2\Phi C_1 & A_2+B_2\Phi(D_1C_2+E_1C_2A_2)\end{bmatrix} \quad (9)$$

where, $\Phi \overset{\text{def}}{=} (I-E_1C_2B_2)^{-1}$.

2) If D_2 is a non-zero matrix, then the derivative of the current cannot be removed and it can now be considered as a new state variable. The derivative of the current can be found by solving (4) as follows

$$di/dt=E_1^{-1}(v-C_1x_1-D_1i) \quad (10)$$

If v is eliminated from the above equation then it becomes a standard state equation, which expresses the derivative in terms of state variables (note i is now a state variable). v can easily be found in (5). Therefore, the state matrix is

$$A_T=\begin{bmatrix}A_1 & 0 & B_1\\ 0 & A_2-B_2D_2^{-1}C_2 & B_2D_2^{-1}\\ -E_1^{-1}C_1 & -E_1^{-1}D_2^{-1}C_2 & E_1^{-1}D_2^{-1}-E_1^{-1}D_1\end{bmatrix} \quad (11)$$

IV. Simulation Results

It should be noted that (4) and (5) are valid, no matter what domain is used for modelling the converter [12], [16]. In this part to show the effectiveness of the method two different systems are studied. The first system is modelled in the *abc* domain, while the other one is modelled in the *dq* domain.

A. Impedance modelling in the abc domain

Fig. 3 shows the power-electronics-based power system considered in this paper, which is based on the CIGRE LV benchmark model [22]. The internal structure and the parameters of the system can be found in Fig. 4 and Table I, respectively. To show the effectiveness of this method even for dealing with numerical models, only the admittances of the converters are used instead of the large transfer functions (the data for this system can be found in [22]). Fig. 5 shows the admittances of 5 converters as a function of frequency. It must be noted that in this part linear converters (the impedance/admittance is in phase domain) are used and these data can easily be imported into commercial softwares, which are capable of power quality calculations. The driving point impedance can easily be calculated at any point by running a harmonic load flow analysis using those softwares.

1) Test Case 1(Inverter 5 is disconnected)

In the first test case Inverter 5 is disconnected at $t=0.2$. The system is divided into two subsystems as shown in Fig. 2, where Subsystem 2 is formed of the grid and Inverter 1 and

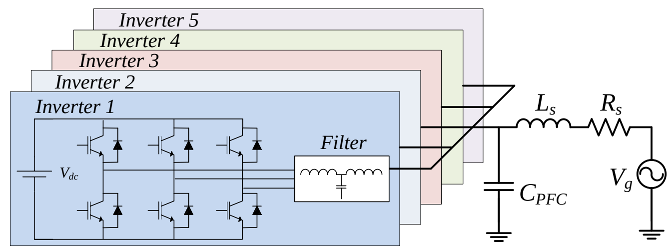

Fig. 3. The multi-converter system considered in this paper, which is based on CIGRE LV benchmark [22].

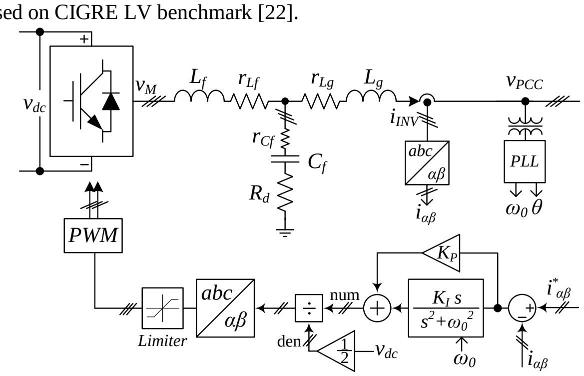

Fig. 4. The internal power circuit and structure of the inverters.

TABLE I. Parameters of the Considered System [22].

Symbol / Description		Inverters 1	2	3	4	5
f_{sw}	Switching/Sampling frequency [kHz]	10		16		10
V_{dc}	DC-link voltage [V]	750				
L_f	Inverter side inductor of the filter [mH]	0.87	1.2	5.1	3.8	0.8
C_f	Filter capacitor [μF]	22	15	2	3	15
L_g	Grid side inductor of the filter [mH]	0.22	0.3	1.7	1.3	0.2
r_{Lf}	Parasitic resistance of L_f [mΩ]	11.4	15.7	66.8	49.7	10
r_{Cf}	Parasitic resistance of C_f [mΩ]	7.5	11	21.5	14.5	11
r_{Lg}	Parasitic resistance of L_g [mΩ]	2.9	3.9	22.3	17	2.5
R_d	Damping resistance [Ω]	0.2	1.4	7	4.2	0.9
K_p	Proportional gain of the controller	5.6	8.05	28.8	16.6	6.5
K_i	Integrator gain of the controller	1000		1500		1000
L_s	Grid inductance [mH]	0.4				
R_s	Grid resistance [Ω]	0.1				

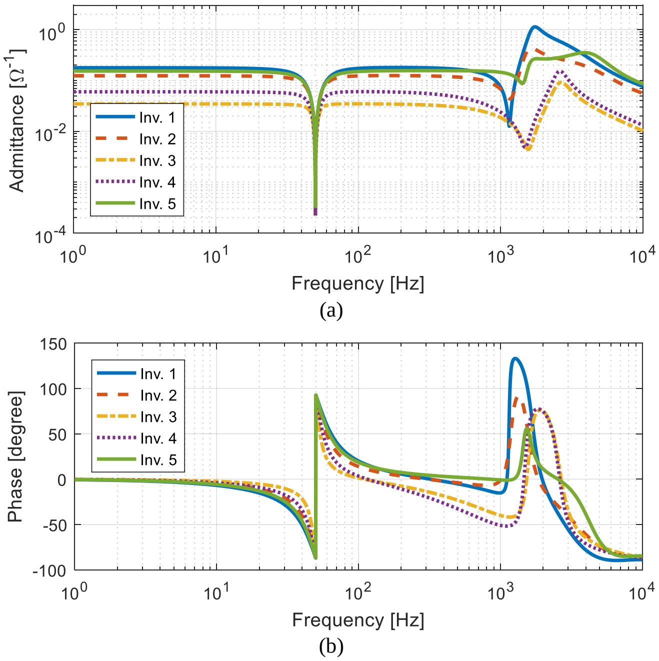

Fig. 5. The admittance characteristics of the converters in Fig. 2: (a) magnitude plot (b) phase plot.

the rest of the system is grouped as Subsystem 1. Fig. 6 shows the results of the VF for different orders, where the maximum error between the original data and approximated model is set to 2%.

It must be noted that this method can also be considered as an order reduction technique. The unimportant dynamics have minimum impact on the frequency response. Therefore, by choosing a proper order for the fitting process, only the important dynamics are considered and it is not necessary to model the entire system, which otherwise leads to very large matrices. For instance, in this case an inverter should at least be modelled as a 6th order transfer function (3 orders for the LCL filter, 2 orders for the resonant controller and at least one order for the delay). This can be seen in Fig. 6 (a). However, a 13th order model (instead of 3x6) is enough for modelling Subsystem 1, which is formed of 3 inverters (Inv. 2, 3 and 4). The same is also true for Subsystem 2, where a 6th order model is enough.

The Nyquist diagram (Subsystem 1 is considered to be the source) as shown in Fig. 7 does not encircle the critical point and one may conclude that the system is stable. However, the time domain results as shown in Fig. 8 reveal that the system is unstable. The reason behind this wrong conclusion is the RHP poles of the minor loop gain. Fig. 9 shows that 2 RHP poles exist in the minor loop gain, which are identified using the VF. In other words, instead of using the sequential methods proposed in [8], [9] to avoid this wrong conclusion, the RHP poles can easily be detected by using the VF in one step.

By using the proposed methodology, the state matrix of the overall closed-loop system can be obtained. The eigenvalues are plotted in Fig. 10, where it can be seen that the instability is because of a pair of eigenvalues, which has positive real parts. The time domain results of Fig. 8 could be used to

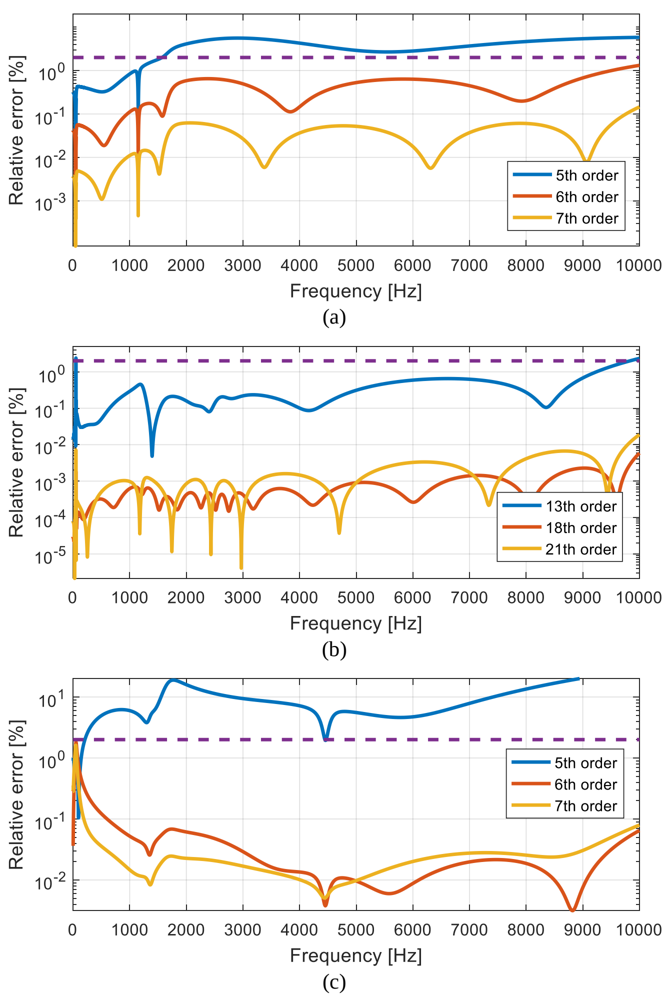

Fig. 6. The results of the VF for (a) Inverter 1 (b) Subsystem 1 and (c) Subsystem 2, with different orders.

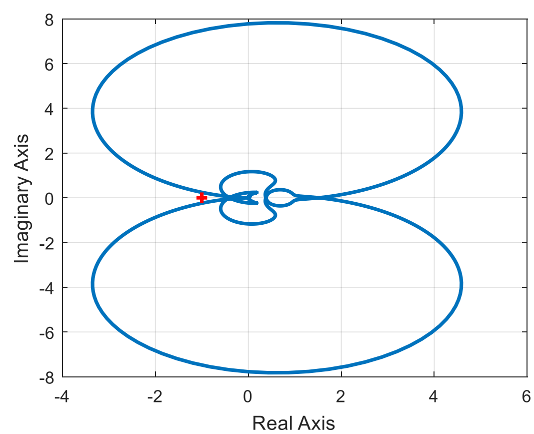

Fig. 7. Nyquist plot of the minor loop gain for Case 1.

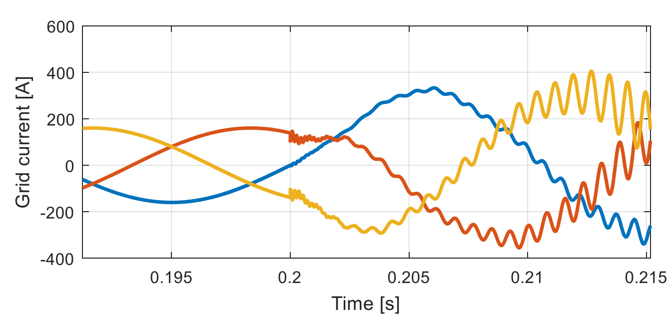

Fig. 8. Time domain results of the unstable case (Case 1).

This article has been accepted for publication in a future issue of this journal, but has not been fully edited. Content may change prior to final publication. Citation information: DOI 10.1109/TEC.2018.2849347, IEEE Transactions on Energy Conversion

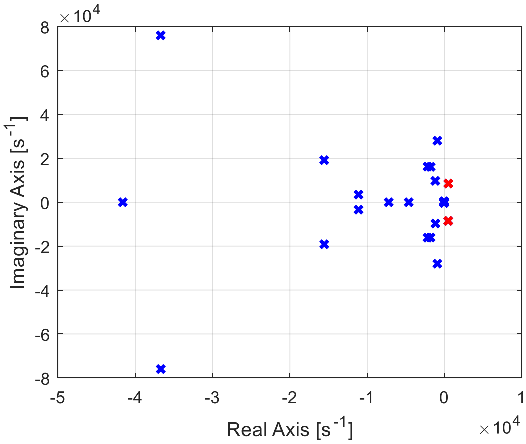

Fig. 9. The minor loop gain has two RHP poles in Case 1.

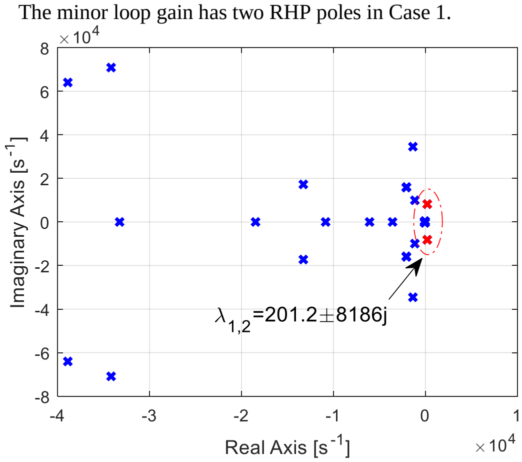

Fig. 10. Two unstable poles exist in the whole closed-loop system.

validate the predicted unstable eigenvalues. Prony analysis very similar to Fourier analysis can be used to find the damping of the frequency components of a transient waveform like Fig. 8 [23].

The results as listed in Table II show a very good correlation with the eigenvalues. The oscillation frequency is almost the same as the imaginary part of the unstable eigenvalue.

Furthermore, the Participation Factor (PF) analysis can be done by some simple matrix operations [13], [24]. For the i^{th} pole, the participation analysis can be done using

TABLE II. RESULTS OF PRONY ANALYSIS FOR CASE 1.

No.	Damping (σ) [1/s]	Frequency (ω) [rad/s]
1	-0.15	314
2	226.8	8200

TABLE III. PARTICIPATION FACTOR ANALYSIS OF THE UNSTABLE POLE OF CASE 1.

Participation Factor	Subsystem
35%	#1
65%	#2

TABLE IV. PARTICIPATION FACTOR ANALYSIS OF THE UNSTABLE POLE OF CASE 1 WITH THE NEW NETWORK DECOMPOSITION.

Participation Factor	Subsystem
50.8%	A
49.2%	B

$$P_{ki} = \frac{\partial \lambda_i}{\partial a_{kk}} = \Phi_{ki}\Psi_{ik} \tag{12}$$

where Φ_i is the right eigenvector of the i^{th} eigenvalue, Ψ_i is the left eigenvector of the i^{th} eigenvalue, and P_{ki} indicates the contribution of the k^{th} state on the i^{th} pole. Since the states are unknown, the sums of participation indices for both subsystems are presented in Table III, which reveals that Subsystem 2 (Grid and Inverter 1) is more responsible for this instability.

In order to find the problematic component more specifically, a different network partitioning can be used. For instance, now consider only Inverter 1 is in Subsystem A and the rest of the system is grouped in Subsystem B. The Participation factor results as shown in Table IV show that Inverter 1 is solely 51% responsible for this instability. Comparing results of Tables III and IV also indicates that the difference in the subsystems, i.e. the grid impedance, is 15% (65%-50%) responsible.

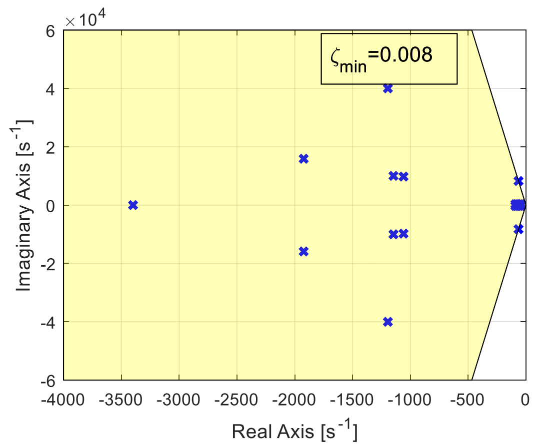

Fig. 11. Eigenvalues of Case 2 (Inverter #3 is disconnected). The minimum damping is highlighted.

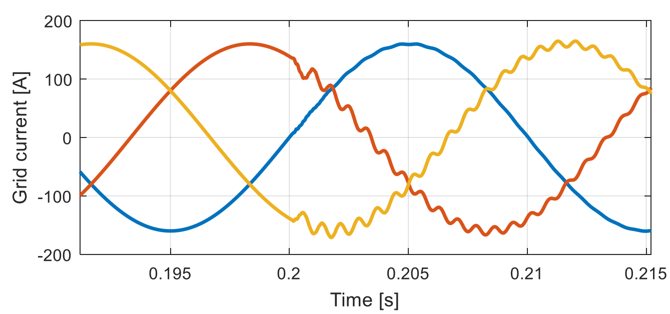

Fig. 12. Time domain results of the stable case (Case 2) after a perturbation.

TABLE V. POLES OF CASE 2 WITH MINIMUM DAMPING.

Eigenvalue	Damping ratio
-6.441e+01 ± 8.254e+03j	0.007804
-1.194e+03 ± 4.003e+04j	0.029824
-1.058e+03 ± 9.785e+03j	0.107577

TABLE VI. RESULTS OF PRONY ANALYSIS FOR CASE 2.

No.	Damping (σ) [1/s]	Frequency (ω) [rad/s]
1	-0.13	314
2	-74.2	8277

This article has been accepted for publication in a future issue of this journal, but has not been fully edited. Content may change prior to final publication. Citation information: DOI 10.1109/TEC.2018.2849347, IEEE Transactions on Energy Conversion

2) Test Case 2 (Inverter 3 is disconnected)

In this case, Inverter 3 is disconnected. The subsystems are the same as Case 1 except Inverter 3 is replaced by Inverter 5. Fig. 11 shows the eigenvalue plot of the system, where no unstable pole can be seen. Time domain results also verify the ability of the system to damp perturbations in the system (see Fig. 12). The frequency and time constant of the transients in the time domain results after a perturbation is almost the same as the frequency and time constant of the lowest damped pole listed in Table V. Results of Prony analysis as shown in Table VI also verify that the dominant pole is identified correctly.

B. Impedance modelling in the dq domain

The *dq* domain is preferred to model converters with outer loop control such as PLL and dc link controller [16], [25], [26]. However, the impedances/admittances are 2×2 matrices instead of scalars, which make the identification process more difficult. In this part, a test case from [16], [27] is considered, which consists of an Active Front End (AFE) and a Voltage Source Inverter (VSI) (see Fig. 13), and the parameters are listed in Table VII. The system is destabilized by changing the integrator gain of the PLL of the VSI as shown in Table VII [27]. The system is decomposed into two subsystems that are highlighted in Fig. 13, where Subsystem 1 is the impedance model and Subsystem 2 is the admittance model. The impedance/ admittance frequency scans of the two subsystems are shown in Fig. 14, where it is clear that the two subsystems are strictly proper (the magnitude goes to zero when the

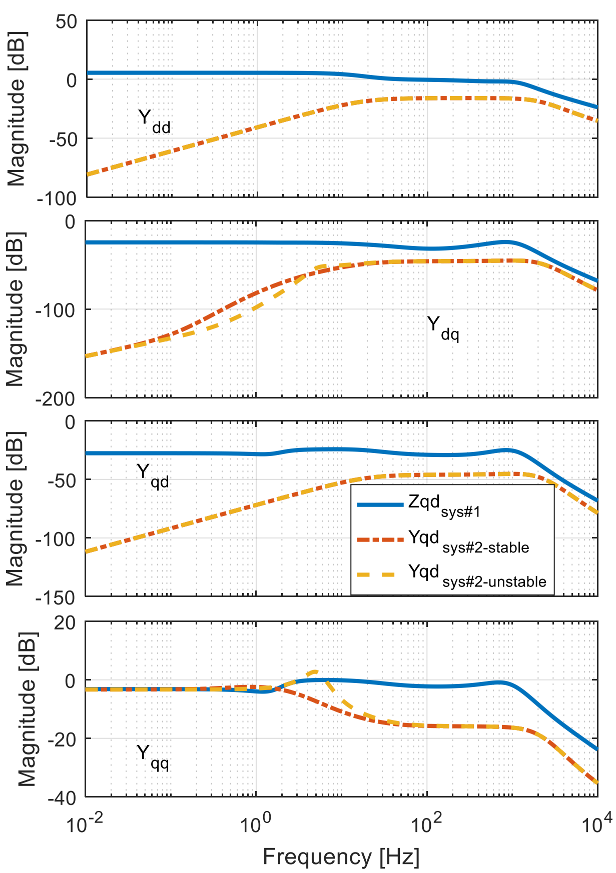

Fig. 14. Frequency scans of the highlighted subsystems in Fig. 13.

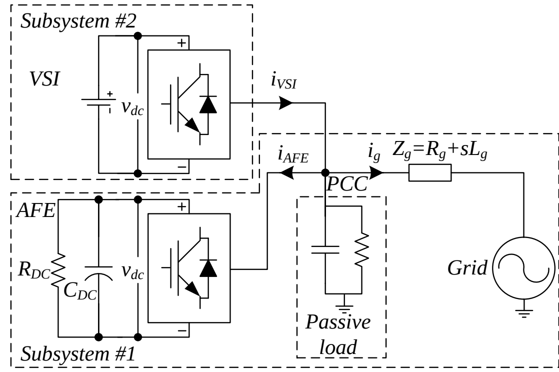

Fig. 13. The considered nonlinear power system with a Voltage Source Inverter (VSI) and an Active Front End (AFE) [16].

frequency tends to infinity).

Fig. 15 shows the results of the proposed method for stable and unstable cases which is almost the same as the results

TABLE VII. PARAMETERS OF THE NONLINEAR POWER SYSTEM [16].

Symbol	Description	Value
	System Parameters	
V_g	Grid voltage (phase voltage rms) [V]	120
f_g	Grid frequency [Hz]	60
R_L	Resistance of local passive load [Ω]	10
C_L	Capacitance of local passive load [μF]	250
L_g	Grid inductance [mH]	0.2
R_g	Grid resistance [Ω]	1.1
	Parameters of the VSI	
L_{VSI}	Inductance of the inverter [mH]	1.0
r_{LVSI}	Self-resistance of L_{VSI} [mΩ]	120
V_{dc}	DC link voltage [V]	600
$i^*_{d\text{-}vsi}$	d channel current reference [A]	140
$i^*_{q\text{-}vsi}$	q channel current reference [A]	0
k_{piVSI}	Proportional gain of current controller	0.0105
k_{iiVSI}	Integrator gain of current controller	1.1519
$k_{pplIVSI}$	Proportional gain of PLL	0.1
$k_{iplIVSI}$	Integrator gain of PLL	0.32 (stable) 5.2 (unstable)
	Parameters of the AFE	
L_{AFE}	Inductance of the AFE [mH]	0.5
r_{LAFE}	Self-resistance of L_{AFE} [mΩ]	90
C_{dcAFE}	Dc link capacitor [μF]	100
R_{dc}	Dc load resistance [Ω]	13.825
V^*_{dc}	DC link voltage reference [V]	600
$i^*_{q\text{-}vsi}$	q channel current reference [A]	0
k_{piAFE}	Proportional gain of current controller	0.0052
k_{iiAFE}	Integrator gain of current controller	1.152
k_{pvAFE}	Proportional gain of dc link voltage controller	0.0628
k_{ivAFE}	Integrator gain of dc link voltage controller	45.45
$k_{pplIVSI}$	Proportional gain of PLL	0.05
$k_{iplIVSI}$	Integrator gain of PLL	0.5
	Common Parameters	
SCF	Signal Conditioning Filter	$\frac{\omega_n^2}{s^2+2\xi\omega_n+\omega_n^2}$
ω_n	Natural frequency of SCF [rad/s]	1.23e6
ξ	Damping factor of SCF [rad/s]	4.74e-13
f_{sw}	Switching/sampling frequency [kHz]	20
T_{del}	Time delay due to the digital control and PWM	$1.5/f_{sw}$

This article has been accepted for publication in a future issue of this journal, but has not been fully edited. Content may change prior to final publication. Citation information: DOI 10.1109/TEC.2018.2849347, IEEE Transactions on Energy Conversion

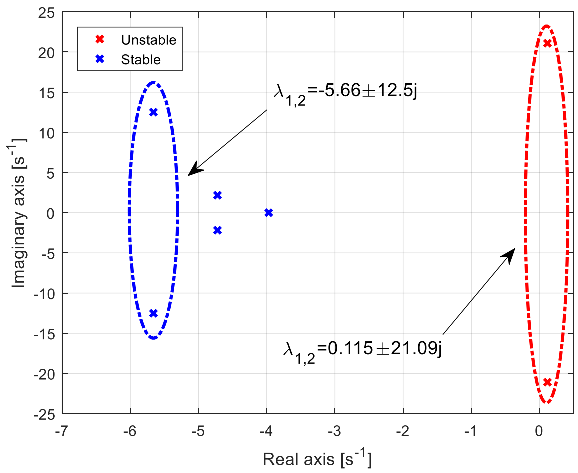

Fig. 15. Eigenvalues of the stable and unstable cases .

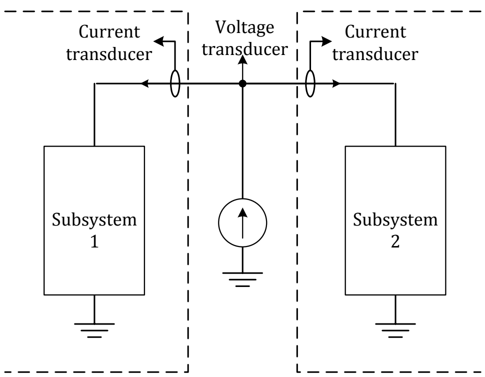

Fig. 16. An impedance measurement system.

obtained and verified in [16].

The participation factor analysis results shown in Table VIII also reveals that Subsystem 1 (VSI) is 75% responsible for the instability while Subsystem 2 (AFE+grid+load) is contributing only 25 %. This is also closely correlated with the results in [16].

C. How to measure impedances/admittances

The impedance measurement systems have widely been discussed in the literature. However, the authors found references [12], [28] interesting. Fig. 16 shows the schematic of such a system. A small signal current with a given frequency is injected into the point of interest either in the *abc* or *dq* domain and then by reading the voltage at that point and the currents towards the subsystems, one can obtain the impedances/admittances of each subsystem at the given frequency.

V. Conclusion

By using the proposed method some difficulties in the impedance based stability evaluation method can be avoided. For instance, the problems of RHP poles in the minor loop gain, which affects the conclusion of the Nyquist stability criterion, can simply be avoided. The relative stability margins such as PM and GM are dependent on the measurement point. However, the proposed method gives the poles of the system, which do not vary based on the measurement point and the relative stability margins can be defined as the minimum

TABLE VIII. Participation Factor Analysis of the Unstable Pole.

Participation Factor	Subsystem
25%	#1
75%	#2

damping of the system. There are also different possibilities for choosing the source and load impedances in a multi-converter system, however, in the proposed method, both subsystems are treated equally. Last but not least, using the participation factor analysis one can identify the root cause of unstable/low-damped poles.

References

[1] J. Sun, “Impedance-Based Stability Criterion for Grid-Connected Inverters,” *IEEE Trans. Power Electron.*, vol. 26, no. 11, pp. 3075–3078, Nov. 2011.

[2] J. Sun, “Small-signal methods for AC distributed power systems-A review,” *IEEE Transactions on Power Electronics*, vol. 24, no. 11, pp. 2545–2554, Nov. 2009.

[3] R. D. Middlebrook, “Input filter design considerations in design and applications of switching regulators,” *Proc. of IEEE Ind. Appl. Soc.Annu. Meeting*, 1976, pp. 91–107.

[4] X. Xiaogang Feng, J. Jinjun Liu, and F. C. Lee, “Impedance specifications for stable DC distributed power systems,” *IEEE Trans. Power Electron.*, vol. 17, no. 2, pp. 157–162, Mar. 2002.

[5] X. Wang, F. Blaabjerg, and W. Wu, “Modeling and Analysis of Harmonic Stability in an AC Power-Electronics-Based Power System,” *IEEE Trans. Power Electron.*, vol. 29, no. 12, pp. 6421–6432, 2014.

[6] M. Amin, M. Molinas, J. Lyu, and X. Cai, “Impact of Power Flow Direction on the Stability of VSC-HVDC Seen from the Impedances Nyquist Plot,” *IEEE Trans. Power Electron.*, vol. 32, no. 10, pp. 8204-8217, Oct. 2017.

[7] K. Ogata, *Modern control engineering*. Prentice Hall, 2002.

[8] C. Yoon, H. Bai, X. Wang, C. L. Bak, and F. Blaabjerg, “Regional modeling approach for analyzing harmonic stability in radial power electronics based power system,” in *Proc. of 2015 IEEE 6th International Symposium on Power Electronics for Distributed Generation Systems, PEDG 2015*, 2015, pp. 1–5..

[9] W. Cao, X. Zhang, Y. Ma, and F. Wang, “Stability criterion and controller parameter design of radial-line renewable systems with multiple inverters,” in *Proc. of IEEE Applied Power Electronics Conference and Exposition - APEC*, 2016, vol. 2016–May, pp. 2229–2236.

[10] C. Buchhagen, M. Greve, A. Menze, and J. Jung, “Harmonic Stability – Practical Experience of a TSO,” in *Proc. of 15th Wind Integration Workshop*, 2016, pp. 1-6.

[11] A. Rygg, M. Amin, M. Molinas, and B. Gustavsen, “Apparent impedance analysis: A new method for power system stability analysis,” in *Proc. of 2016 IEEE 17th Workshop on Control and Modeling for Power Electronics (COMPEL)*, 2016, pp. 1–7.

[12] A. Rygg and M. Molinas, “Apparent impedance analysis: A small-signal method for stability analysis of power electronic based systems,” *IEEE J. Emerg. Sel. Top. Power Electron.*, vol. 5, no. 4, pp. 1474–1486, 2017.

[13] Y. Wang, X. Wang, F. Blaabjerg, and Z. Chen, “Harmonic Instability Assessment Using State-Space Modeling and Participation Analysis in Inverter-Fed Power Systems,” *IEEE Trans. Ind. Electron.*, vol. 64, no. 1, pp. 806-816, Jan. 2017.

[14] M. K. Bakhshizadeh, F. Blaabjerg, J. Hjerrild, X. Wang, L. Kocewiak, and C. L. Bak, “A Numerical Matrix-Based Method for Stability and Power Quality Studies Based on Harmonic Transfer Functions,” *IEEE J. Emerg. Sel. Top. Power Electron.*, vol. 5, no. 4, pp. 1542–1552, 2017.

[15] M. K. Bakhshizadeh, F. Blaabjerg, C. Leth Bak, F. Faria da Silva, J. Hjerrild, K. Lukasz, B. Hesselbaek, and T. Sørensen, “Harmonic Modelling, Propagation and Mitigation for Large Wind Power Plants Connected via Long HVAC Cables: Review and Outlook of Current

This article has been accepted for publication in a future issue of this journal, but has not been fully edited. Content may change prior to final publication. Citation information: DOI 10.1109/TEC.2018.2849347, IEEE Transactions on Energy Conversion

Research," in *Proc. of IEEE ENERGYCON 2016*, 2016, pp. 1–5.

[16] M. K. Bakhshizadeh, C. Yoon, J. Hjerrild, C. L. Bak, L. Kocewiak, F. Blaabjerg, and B. Hesselbaek, "The Application of Vector Fitting to Eigenvalue-based Harmonic Stability Analysis," *IEEE J. Emerg. Sel. Top. Power Electron.*, vol. 5, no. 4, pp. 1487–1498, 2017.

[17] B. Gustavsen and A. Semlyen, "Rational approximation of frequency domain responses by vector fitting," *IEEE Trans. Power Deliv.*, vol. 14, no. 3, pp. 1052–1061, Jul. 1999.

[18] B. Gustavsen, "Improving the Pole Relocating Properties of Vector Fitting," *IEEE Trans. Power Deliv.*, vol. 21, no. 3, pp. 1587–1592, Jul. 2006.

[19] D. Deschrijver, M. Mrozowski, T. Dhaene, and D. De Zutter, "Macromodeling of multiport systems using a fast implementation of the vector fitting method," *IEEE Microw. Wirel. Components Lett.*, vol. 18, no. 6, pp. 383–385, Jun. 2008.

[20] B. Gustavsen and A. Semlyen, "Enforcing passivity for admittance matrices approximated by rational functions," *IEEE Trans. Power Syst.*, vol. 16, no. 1, pp. 97–104, Feb. 2001.

[21] L. Harnefors, X. Wang, A. G. Yepes, and F. Blaabjerg, "Passivity-Based Stability Assessment of Grid-Connected VSCs—An Overview," *IEEE J. Emerg. Sel. Top. Power Electron.*, vol. 4, no. 1, pp. 116–125, Mar. 2016.

[22] C. Yoon, H. Bai, R. N. Beres, X. Wang, C. L. Bak, and F. Blaabjerg, "Harmonic Stability Assessment for Multiparalleled, Grid-Connected Inverters," *IEEE Trans. Sustain. Energy*, vol. 7, no. 4, pp. 1388–1397, Oct. 2016.

[23] J. F. Hauer, "Application of Prony analysis to the determination of modal content and equivalent models for measured power system response," *IEEE Trans. Power Syst.*, vol. 6, no. 3, pp. 1062–1068, Aug. 1991.

[24] P. Kundur, *Power system stability and control*. McGraw-Hill, 1994.

[25] M. K. Bakhshizadeh, X. Wang, F. Blaabjerg, J. Hjerrild, L. Kocewiak, C. L. Bak, and B. Hesselbek, "Couplings in Phase Domain Impedance Modelling of Grid-Connected Converters," *IEEE Trans. Power Electron.*, vol. 31, no. 10, pp. 6792–6796, 2016.

[26] A. Rygg, M. Molinas, Z. Chen, and X. Cai, "A modified sequence domain impedance definition and its equivalence to the dq-domain impedance definition for the stability analysis of AC power electronic systems," *IEEE J. Emerg. Sel. Top. Power Electron.*, vol. 4, no. 4, pp. 1383–1396, 2016.

[27] B. Wen, D. Dong, D. Boroyevich, R. Burgos, P. Mattavelli, and Z. Shen, "Impedance-Based Analysis of Grid-Synchronization Stability for Three-Phase Paralleled Converters," *IEEE Trans. Power Electron.*, vol. 31, no. 1, pp. 26–38, Jan. 2016.

[28] G. Francis, R. Burgos, D. Boroyevich, F. Wang, and K. Karimi, "An algorithm and implementation system for measuring impedance in the D-Q domain," in *Proc. Of 2011 IEEE Energy Conversion Congress and Exposition*, 2011, pp. 3221–3228.

Mohammad Kazem Bakhshizadeh (S'16) received the B.S. and M.S. degrees in electrical engineering from the Amirkabir University of Technology, Tehran, Iran in 2008 and 2011, respectively. He is currently an industrial PhD student at Aalborg University, Aalborg, Denmark in collaboration with DONG Energy Wind Power, Fredericia, Denmark. In 2016, he was a visiting scholar at Imperial College London, London, U.K. His research interests include power quality, modeling and control of power converters, and grid converters for renewable energy systems.

Frede Blaabjerg (S'86–M'88–SM'97–F'03) was with ABB-Scandia, Randers, Denmark, from 1987 to 1988. From 1988 to 1992, he got the PhD degree in Electrical Engineering at Aalborg University in 1995. He became an Assistant Professor in 1992, an Associate Professor in 1996, and a Full Professor of power electronics and drives in 1998. From 2017 he became a Villum Investigator.

His current research interests include power electronics and its applications such as in wind turbines, PV systems, reliability, harmonics and adjustable speed drives. He has published more than 450 journal papers in the fields of power electronics and its applications. He is the co-author of two monographs and editor of 6 books in power electronics and its applications.

He has received 18 IEEE Prize Paper Awards, the IEEE PELS Distinguished Service Award in 2009, the EPE-PEMC Council Award in 2010, the IEEE William E. Newell Power Electronics Award 2014 and the Villum Kann Rasmussen Research Award 2014. He was the Editor-in-Chief of the IEEE TRANSACTIONS ON POWER ELECTRONICS from 2006 to 2012. He has been Distinguished Lecturer for the IEEE Power Electronics Society from 2005 to 2007 and for the IEEE Industry Applications Society from 2010 to 2011 as well as 2017 to 2018.

He is nominated in 2014, 2015 and 2016 by Thomson Reuters to be between the most 250 cited researchers in Engineering in the world. In 2017 he became Honoris Causa at University Politehnica Timisoara (UPT), Romania.

Jesper Hjerrild was born in 1971. He holds an MSc and PhD degrees in electrical engineering from the Technical University of Denmark, Lyngby, in 1999 and 2002, respectively. Currently, he is employed with DONG Energy. His main technical interest is electrical power systems in general, involving a variety of technical disciplines including modeling of power system including wind power and power system control, stability and harmonics. Furthermore, he also works with designing of the wind farm.

Łukasz Hubert Kocewiak (M'12, SM'16) holds BSc and MSc degrees in electrical engineering from Warsaw University of Technology as well as PhD degree from Aalborg University.

Currently he is with Ørsted Wind Power and is working as an R&D manager and senior power system engineer on development of electrical infrastructure in large offshore wind power plants.

The main direction of his research is related to harmonics and nonlinear dynamics in power electronics and power systems especially focused on wind power generation units.

He is the author/co-author of more than 60 publications. He is a member of various working groups within Cigré, IEEE, IEC.

Claus Leth Bak was born in Århus, Denmark, on April 13th, 1965. He received the B.Sc. with honors in Electrical Power Engineering in 1992 and the M.Sc. in Electrical Power Engineering at the Department of Energy Technology at Aalborg University in 1994. After his studies he worked as a professional engineer with Electric Power Transmission and Substations with specializations within the area of Power System Protection at the NV Net Transmission System Operator. In 1999 he was employed as an Assistant Professor at the Department of Energy Technology, Aalborg University, where he holds a Full Professor position today. He received the PhD degree in 2015 with the thesis "EHV/HV underground cables in the transmission system". He has supervised/co-supervised +35 PhD's and +50 MSc theses. His main Research areas include Corona Phenomena on Overhead Lines, Composite Transmission Towers, Power System Modeling and Transient Simulations, Underground Cable transmission, Power System Harmonics, Power System Protection and HVDC-VSC Offshore Transmission Networks. He is the author/coauthor of app. 290 publications. He is a member of Cigré SC C4 AG1 and SC B5 and chairman of the Danish Cigré National Committee (August 2018). He is an IEEE senior member (M'1999, SM'2007). He received the DPSP 2014 best paper award and the PEDG 2016 best paper award. He serves as Head of the Energy Technology PhD program (+ 100 PhD's) and as Head of the Section of Electric Power Systems and High Voltage and is a member of the PhD board at the Faculty of Engineering and Science.